

Obtaining an intermediate band photovoltaic material through the Bi insertion in CdTe

Y. Seminovski ¹, P. Palacios ², P. Wahnón ¹

ABSTRACT

Defect interaction can take place in CdTe under Te and Bi rich conditions. We demonstrate in this work through first principles calculations, that this phenomenon allows a Jahn Teller distortion to form an isolated half-filled intermediate band in the host semiconductor band-gap. This delocalized energy band supports the experimental deep level reported in the host band-gap of CdTe at a low bismuth concentration. Furthermore, the calculated optical absorption of CdTe:Bi in this work shows a significant subband-gap absorption that also supports the enhancement of the optical absorption found in the previous experimental results.

1. Introduction

Enhanced efficiency in an intermediate band (IB) solar cell is obtained through the absorption of extra photons of the incident radiation [1]. It is predicted that an isolated, delocalized band is located inside the doped semiconductor band-gap, forming a partially occupied energy level. This IB promotes two additional electrons to the unoccupied bands, increasing the photon absorption of the doped solid. The voltage is gained by the host semiconductor band-gap while the photocurrent is increased. A high current density is obtained which enhances the whole IB solar cell efficiency. It was previously reported that an IB is formed through the spatial symmetry of the non-bonded d orbitals of a transition metal dopant. Using this hypothesis several doped semiconductors have been proposed as candidates in the manufacture of IB solar cells [2–6].

Among the photovoltaic materials used, CdTe is one of the most promising. The structure and electronegativity of the atoms in CdTe permit the formation of a neither-ionic nor-covalent bond that yields a direct band-gap not far from the optimum band-gap for the conversion efficiency [7]. Previously, several experimental results demonstrated that CdTe doped with Bi can enhance, in

some cases, the photon absorption of the incident solar radiation [8,9].

With the growth of CdTe cadmium vacancies V_{Cd} [11] appear to act like acceptor centers, which are the predominant defects under Te rich conditions. The V_{Cd} in the Te and Bi rich condition has been experimentally found negatively and double negatively charged at $E_V+0.14$ eV and $E_V+0.38$ eV respectively [8] and with a concentration ranging from around $10^{17}-10^{18}$ cm^{-3} . Furthermore in the undoped CdTe, it is demonstrated that in the Cd rich condition interstitial Cd, Cd_i , are the dominant defects [12,13].

Bismuth Bi, having a metal behavior, high carrier mobility and low effective masses, is a widely used dopant. When Bi is inserted into a CdTe semiconductor, a deep level at $E_V+0.71$ eV is reported [8]. Different hypotheses have been proposed to explain this deep level in CdTe:Bi. Saucedo et al. [9] states that Bi introduced into CdTe and in a Cd position (Bi_{Cd}) compensates the V_{Cd} and forms the semi-insulating CdTe when a tetrahedral to octahedral distortion is induced, and consequently Te atoms are displaced forming two Te–Te dimers around the Bi_{Cd} . We calculated, using Density Functional Theory (DFT), the formation energy of a model supercell containing two Te–Te dimers around Bi_{Cd} [10]. The results of this simulation demonstrated that the Te–Te configurational equilibration position is far from a dimer formation in these conditions and instead a simple Bi_{Cd} substitution without structural distortion appears. This theoretical result is different from the prediction of Saucedo et al. [9], but a tetrahedral to octahedral distortion is in fact what should happen in CdTe:Bi.

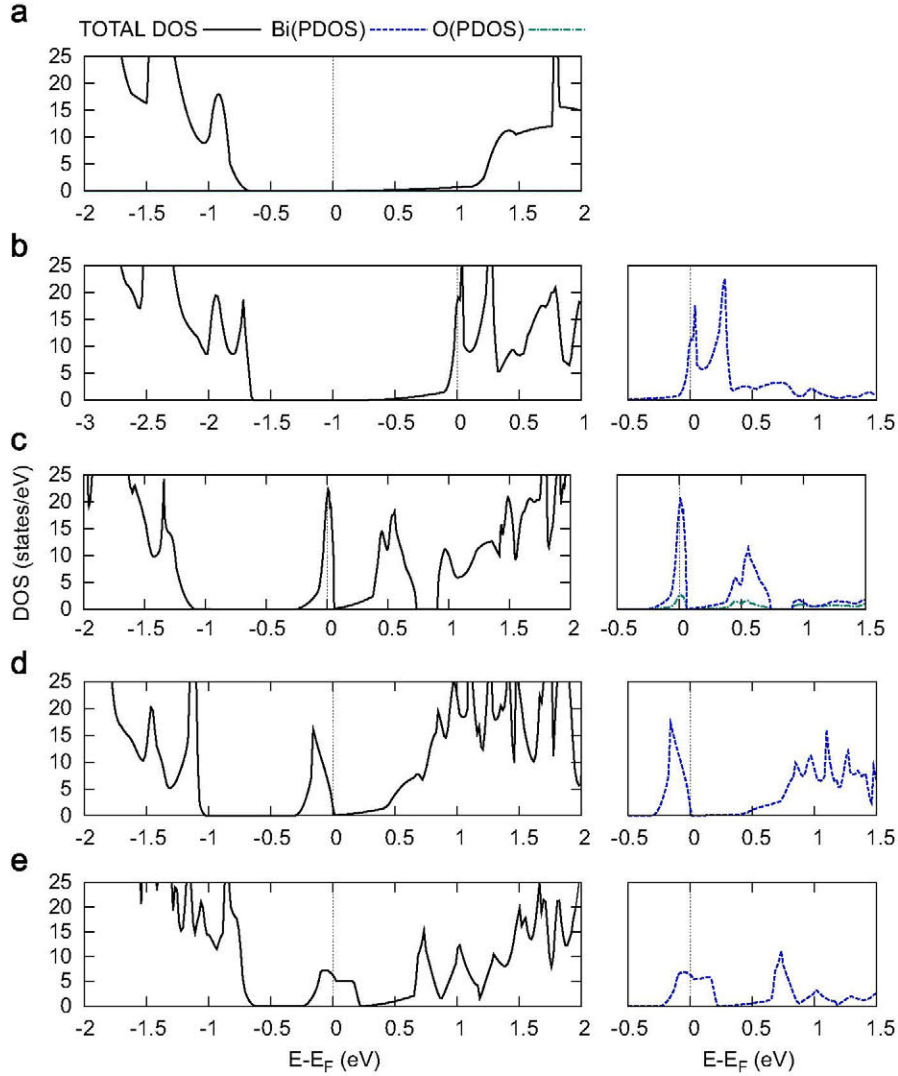


Fig. 1. DOS of (a) the host semiconductor CdTe. (b)-(e) CdTe:Bi in different situations: (b) $\text{BiCd}_{15}\text{Te}_{16}$ (Bi_{Cd}), (c) $\text{OBiCd}_{15}\text{Te}_{15}$ ($\text{Bi}_{\text{Cd}}+\text{O}_{\text{Te}}$), (d) $\text{Bi}_2\text{Cd}_{14}\text{Te}_{16}$ (2Bi_{Cd}), (e) $\text{BiCd}_{15}\text{Te}_{16}$ ($\text{Bi}_i+\text{V}_{\text{Cd}}$). PDOS in PAW spheres and in arbitrary units qualitatively demonstrate the position of the Bi orbital contribution.

Du [14] points out that Bi in CdTe located at the Cd position and interacting with oxygen substituting tellurium ($\text{Bi}_{\text{Cd}}+\text{O}_{\text{Te}}$) adopts a C_{3v} symmetry that is coherent with a Jahn Teller distortion [15]. This result implies a high oxygen co-doping. However, these aforementioned experiments [8,9] are made restricting oxygen concentration range to the 10^{14} - 10^{15} cm^{-3} level [16]. Therefore this cannot be the explanation.

Furthermore, it is predictable under the Te and Bi rich condition that the dominant defects are the interstitial bismuth atoms Bi_i and V_{Cd} with the possibility of defect compensation in a long range interaction. The probability of Bi_i as a dominant defect is predicted analogue to the case of a Cd rich condition in undoped CdTe where Cd_i is the dominant defect.

A CdTe zinc blend structure has 3 interstitial sites in the $\langle 111 \rangle$ direction: 2 tetrahedral and 1 octahedral the $\langle 111 \rangle$ is the preferential direction of the interstitial defect movement. Previous works have found that Bi spontaneously diffuses throughout the CdTe lattice [8,9] but as Bi is a big atom to be placed in the interstices, the diffusion coefficient of Bi in CdTe cannot be determined. The explanation of this phenomenon by Hage-Ali et al. [17] is consistent with a complex defect formation in which V_{Cd} and Bi_i should be addressed. These authors also compared the diffusion mechanism in CdTe:Bi with that of the Cu doped Ge

[18], thus the existence of Bi inside CdTe in the Cd position or displaced to an interstitial site and interacting with V_{Cd} depends on the concentration of V_{Cd} .

In the present work, using first principles calculations, a defect interaction between some important defects in CdTe demonstrates a distortion that breaks the symmetry of the orbitals and separates some states in the middle of the gap which can be related to the deep level previously found experimentally.

2. Computational details

The calculations were made using DFT, implemented in *Vienna Ab-initio Simulation Package* (VASP) [19,20] code, in the Perdew-Burke-Ernzerhof [21] parametrization of the generalized gradient approximation [22] and using projector augmented waves (PAWs) [23,24]. All the parameters were tested to obtain accurate convergence in each case.

The electronic calculations were made by increasing the k-points grid in order to obtain accurate results. The method used in this case was the linear tetrahedron method as implemented in the VASP code.

The partial contributions to the optical absorption were obtained through the product of weighted imaginary part ϵ_2 of the total dielectric function and the energy of the different direct transitions in each band. The dielectric function is multiplied by the energy giving a weighted result that allows the comparison of the partial contribution of the different direct transitions in each band. The separation of the occupancies by bands permits the obtainment of the optical absorption in order to compare with the experimental one, despite the subestimation of the band-gap in the GGA method. We used the HSE06 screened hybrid functional [25,26] to obtain each gap, from valence band (VB) to the IB and from IB to conduction band CB. The results were used to apply a scissor shift to the result of the weighted imaginary part ϵ_2 of total dielectric function and partial contribution of the different direct transitions in each band [27]. This scissor shift permits the correct absorption coefficient related with gaps in CdTe:Bi to be obtained.

3. Results and discussion

The different possibilities of the predicted dominant defects that can appear in CdTe:Bi under Te and Bi rich conditions were calculated. These defects are: Bi_{Cd} , and the interacting defects $\text{Bi}_{\text{Cd}}+\text{O}_{\text{Te}}$, interaction of two Bi_{Cd} 2Bi_{Cd} and finally $\text{Bi}_i+\text{V}_{\text{Cd}}$.

Table 1
Bi-Te distances $d_{\text{Bi-Te}}$, Bi-O distances $d_{\text{Bi-O}}$, Te:Bi:Te angles $\angle_{\text{Te:Bi:Te}}$ and Te:Bi:O angles $\angle_{\text{Te:Bi:O}}$ of the final obtained structures.

Defect type	$d_{\text{Bi-Te}}$ (Å)	$d_{\text{Bi-O}}$ (Å)	$\angle_{\text{Te:Bi:Te}}$ (°)	$\angle_{\text{Te:Bi:O}}$ (°)
Bi_{Cd}	3.07	-	109.6	-
$\text{Bi}_{\text{Cd}}+\text{O}_{\text{Te}}$	3.01	2.49	93.6	128.4
2Bi_{Cd}	3.04-3.25	-	90.4-121.3	-
$\text{Bi}_i+\text{V}_{\text{Cd}}$	2.94-3.47	-	118.2	-

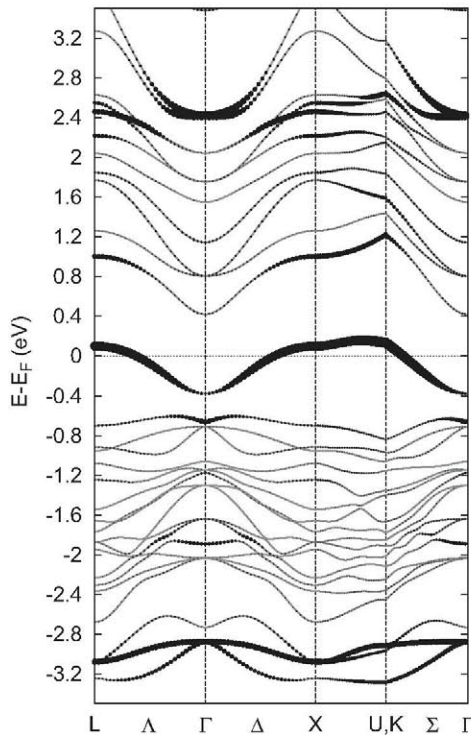


Fig. 2. Band diagram of the $\text{Bi}_i+\text{V}_{\text{Cd}}$ defect compensation in a 16 atom CdTe:Bi cell. (Dark dots represent the Bi 6p orbital projections in the PAW spheres).

The resulting densities of states (DOSs) and projected densities of states (PDOSs) of Bi in all of the doped cases (and O in $\text{Bi}_{\text{Cd}}+\text{O}_{\text{Te}}$ case) were obtained (Fig. 1). The dopant levels can be seen in the band-gap vicinity if we compare the DOS of the doped supercells with that of the host CdTe semiconductor. When Bi substitutes the Cd in the CdTe structure (Fig. 1(b)) the excess electron added by Bi raises the Fermi energy level to the conduction band. The result is an n-type doping which is not consistent with the formation of a semi-insulating material found experimentally. Then if an stoichiometric amount of oxygen O is added (Fig. 1(c)) a Jahn Teller distortion appears as expected [14]. The O electro-negativity being higher than that of Te stabilizes the Bi levels producing new states below the Te-related conduction band, and at the same time the O imposes an attraction to the neighboring Bi atom. The result is a distorted structure with a semi-occupied Bi level having the excess electron band separated from the conduction band. In the interacting 2Bi_{Cd} (Fig. 1(d)) a deformation product of a Bi atom repulsed by steric hindrance appears. The resulting deformed structure has the Bi DOS separated from the rest and containing the excess two electrons. Finally the Bi_i interacting with V_{Cd} (Fig. 1(e)) also deforms the structure when the two are in a long-range interaction, the resulting DOS forms an isolated partially filled IB having the excess electron. The Bi PDOS in the cases of the interacting defects demonstrated that the Jahn Teller distortion breaks the symmetry of the contribution of 6p Bi orbitals and separates part of the hybridized levels in the formed structure, but the separation of the Bi levels in Bi PDOS of the Bi_{Cd} case cannot be seen.

Table 1 contains the obtained Bi-Te distances (and Bi-O distance in $\text{Bi}_{\text{Cd}}+\text{O}_{\text{Te}}$ case) and Te:Bi:Te angles (and Te:Bi:O angles in $\text{Bi}_{\text{Cd}}+\text{O}_{\text{Te}}$ case). The CdTe bond distance is approximately 2.8 Å and a relaxation to higher values can be seen in all cases. All the Bi-Te distances in the Bi_{Cd} case are higher but identical and this does not lead to a distortion in the cell because the Te:Bi:Te angle in this case remains identical to that of the former structure. The distorted final structures around the Bi in $\text{Bi}_{\text{Cd}}+\text{O}_{\text{Te}}$, 2Bi_{Cd} and $\text{Bi}_i+\text{V}_{\text{Cd}}$ also goes to higher but different values and the tetrahedral angles go from 109.4° to different values by the distortion provoked by defect interactions. The Bi-O distances are lower than those of the CdTe host lattice, which is coherent with the attraction that appears among the Bi and O, also the Bi-O bond is stronger than the Bi-Te or O-Cd of the surrounding structure.

The case of $\text{Bi}_i+\text{V}_{\text{Cd}}$ that forms the IB presents a defect compensation that occurs along the $\langle 111 \rangle$ in the C_{3v} -axis. In Fig. 2 the PBE band diagram along the direction of maximum symmetry k-points of the corresponding CdTe 216 spatial group can be observed. In this figure the Bi 6p orbital projections over the PAW spheres can also be observed. The IB is made up of one delocalized electron in the Bi 6p outer shell orbital.

The Fermi energy level is located in the intermediate band but the Γ point has an energy which is the lowest in the IB. This is because the host band-gap is direct and has a great dispersion at the Γ point that forms a deep minimum in the conduction band. The Bi levels included also form a same band dispersion in the IB due to the interaction with V_{Cd} .

The surrounding Te atoms have non-compensated bonds near the V_{Cd} zone and the Bi atom with 6p³ outer shell compensates the Te bonds, probably hybridized with the Te 5p outer shell orbitals. This forms a bonding band deep within the valence band that also has the anti-bonding part around 3 eV over the Fermi level shown with the Bi 6p orbital projections in Fig. 2.

A resulting Jahn Teller distortion occurs but only when the Bi atom is located in the interstitial site Bi_i in a long range interaction instead of the substitutional case Bi_{Cd} . The deformed obtained structure still has a trigonal symmetry, having a C_{3v} -axis along the $\langle 111 \rangle$ direction. It is demonstrated that a Bi_xTe_y

spontaneously appears when CdTe is doped with Bi [14]. The 3 Te that are near the Bi atom form a 118.2° angle near the 120° trigonal angles, preventing the adoption of the correct geometry configuration that forms a Bi_xTe_y .

A subsequent calculation using the Heyd-Scuseria-Ernzerh of (HSE06) [25,26] screened hybrid functional was applied after the PBE geometry optimization to obtain more accurate subband-gaps. The resulting valence-intermediate (VB-IB) and intermediate-conduction (IB-CB) subband-gaps at the Γ point obtained were 0.42 eV and 1.29 eV respectively.

In Fig. 3(a) it can be observed that the optical absorption α of CdTe:Bi having the $\text{Bi}_i + V_{\text{Cd}}$ interaction, is higher than the α of the CdTe host semiconductor. The α of the IB is obtained by applying a corresponding scissor shift [27] using the subband-gaps that we obtained from the HSE06 calculation at the Γ point. This shift was applied to the VB-IB and IB-CB transitions. In the case of valence band to intermediate band (VB-CB) transitions the scissor shift applied corresponds to the band-gap obtained after an HSE06 calculation of the CdTe host. The gained photon absorption can also be observed with the increase in the partial contributions to the optical absorption in Fig. 3(b).

3.1. $\text{Bi}_i + V_{\text{Cd}}$ and the intermediate band formation in CdTe:Bi

The experimental conditions that could favor the Bi complex in the synthesis of CdTe:Bi includes the formation of an extended concentration of cadmium vacancies. As has been theoretically

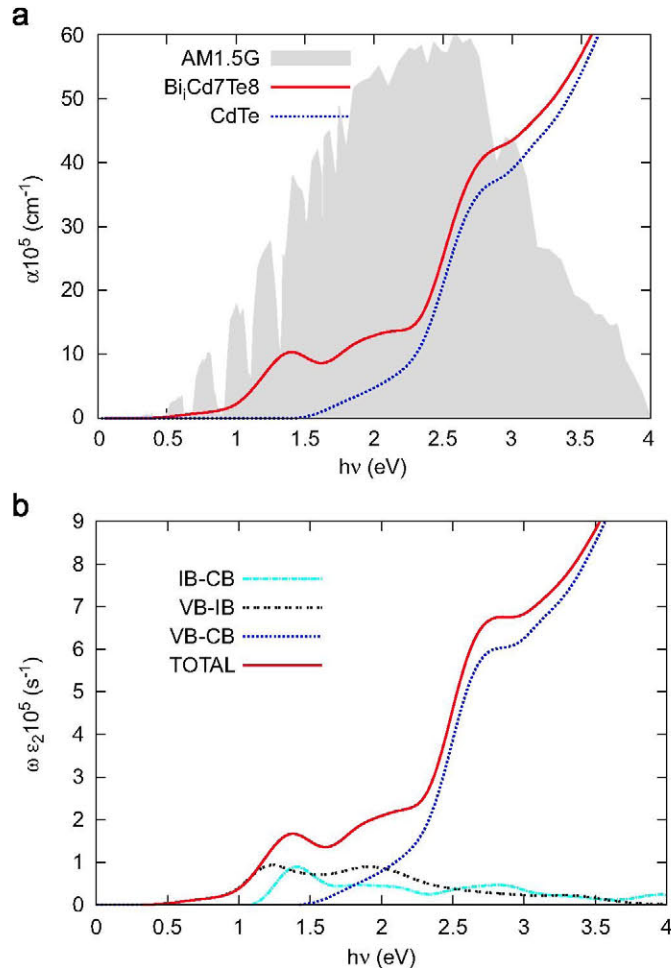


Fig. 3. (a) Corresponding optical absorption and (b) weighted imaginary part ϵ_2 of the total dielectric function and the partial contribution of the different direct transitions to it.

described in Table 2, Bi in Cd position is more favored than Bi in interstitial sites. The stabilization of V_{Cd} defects with low formation energy [28] greatly favors the stabilization of Bi in an interstice of CdTe lattice and the consequent IB formation.

The experimental findings on the position of Bi in CdTe are not completely understood yet. In fact, it is not clear that Bi is actually located in Cd positions and the deep level identified at $E_V + 0.71$ eV, that is related to the enhanced photon absorption cannot be explained as a hole trap. Instead an IB is an approach to discuss the enhanced photon absorption that appears in this case. An IB through the delocalization of electrons avoids rapid recombination and/or a hole trap formation.

Furthermore, Bi is a big atom and steric hindrance can appear after stabilization of Bi in Cd position. The valence of Bi (3) different from that of Cd (2) is an added argument to produce a new material with a different symmetrical order (Fig. 4). The extended Bi 6p orbital forms a “disconnected” delocalized band that contains one electron per Bi atom half filling this orbital and giving space to the excitation of new electrons. This delocalized band, extended into a different symmetrical order, avoids losses through its partial dispersion and perfect isolation from the other bands.

Table 2
CdTe:Bi energetics. Relative energy E_{rel} of Bi displaced from Cd position forming a Bi-complex $\text{Bi}_i + V_{\text{Cd}}$ in relation with the corresponding energy of Bi in Cd position, Bi_{Cd} .

Defects	E_{rel} (eV)
Bi_{Cd}	0
$\text{Bi}_i + V_{\text{Cd}}$	1.43

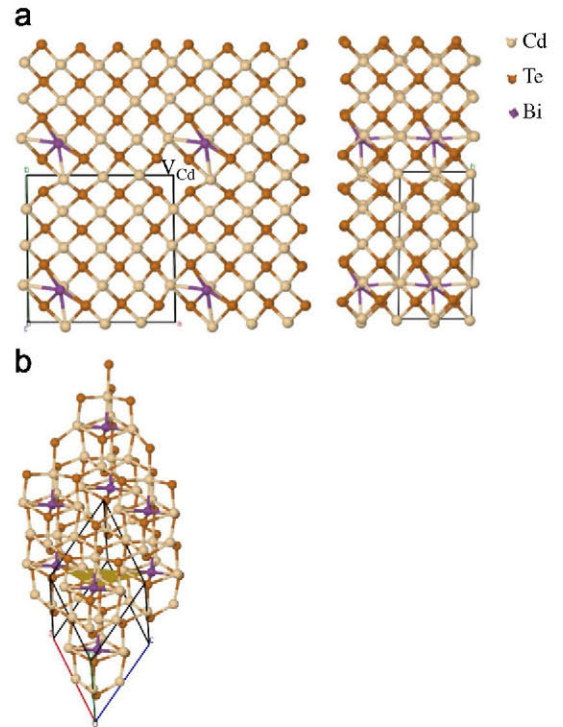


Fig. 4. A $2 \times 2 \times 2$ expansion of the structure obtained in (a) a 32 atoms supercell along the direction of the defect line, the positions of cadmium vacancy, V_{Cd} are also observed and (b) a 16 atom supercell with rhomboedric axis, the V_{Cd} is represented by the trigonal area along the surrounding Bi atoms.

4. Conclusions

A CdTe lattice with V_{Cd} and having Bi impurity forms a stable compound in a distorted cell, which should correspond to the experimental findings. A structure containing Bi in a Cd position does not have distortion and a simple n-type doping is the result. Bi interacting with O demonstrates a Jahn Teller distortion that inserts in the gap states separated from the conduction band minimum. The Bi states appear semi-filled in the middle of the host semiconductor band-gap. $2Bi_{Cd}$ presents a repulsion among the Bi atoms and the resulting distortion breaks the symmetry of the p orbitals and the excess electron appears in separated densities of states, forming a completely filled IB. The mechanism of one or the other defect interactions in the CdTe is dependent on V_{Cd} , Bi_i , O_{Te} and Bi_{Cd} concentrations and the distances between them. A partially filled and isolated IB in the mid-gap of the host CdTe, is formed when a complex defect Bi_i+V_{Cd} appears. The experimental deep level found at $E_V+0.71$ eV corresponds to the formation of this partially delocalized and partially dispersed band that is located in the middle of the band gap of the host semiconductor, resulting from the Bi_i+V_{Cd} complex defect formation.

Acknowledgment

We wish to thank Professor J.C. Conesa for his critical reading of the manuscript. We would like to acknowledge the funding from the FOTOMAT project (Grant no. MAT2009-14625-C03-01) and the Comunidad de Madrid NUMANCIA2 project (S-2009ENE-1477). Authors thankfully acknowledge the computer resources, technical expertise and assistance provided by the Centro de Supercomputación y Visualización de Madrid (CeSViMa) and the Spanish Supercomputing Network.

References

- [1] A. Luque, A. Martí, Increasing the efficiency of ideal solar cells by photon induced transitions at intermediate levels, *Physical Review Letters* 78 (1997) 5014–5017.
- [2] P. Wahnón, C. Tablero, *Ab initio* electronic structure calculations for metallic intermediate band formation in photovoltaic materials, *Physical Review B* 65 (2002) 165115-1–165115-10.
- [3] P. Palacios, K. Sánchez, J.C. Conesa, P. Wahnón, First principles calculation of isolated intermediate bands formation in a transition metal-doped chalcopyrite-type semiconductor, *Physica Status Solidi A* 203 (6) (2006) 1395–1401.
- [4] K. Sánchez, I. Aguilera, P. Palacios, P. Wahnón, Assessment through first-principles calculations of an intermediate-band photovoltaic material based on Ti-implanted silicon: interstitial versus substitutional origin, *Physical Review B* 79 (2009) 165203-1–165203-7.
- [5] P. Palacios, I. Aguilera, K. Sánchez, J.C. Conesa, P. Wahnón, Transition-metal-substituted indium thiospinels as novel intermediate-band materials: prediction and understanding of their electronic properties, *Physical Review Letters* 101 (2008) 046403-1–046403-4.
- [6] P. Wahnón, J.C. Conesa, P. Palacios, R. Lucena, I. Aguilera, Y. Seminovski, F. Fresno, V-doped SnS₂: a new intermediate band material for a better use of the solar spectrum, *Physical Chemistry Chemical Physics* 13 (2011) 20401.
- [7] W. Shockley, H.J. Queisser, Detailed balance limit of efficiency of p–n junction solar cells, *Journal of Applied Physics* 32 (3) (1961) 510–519.
- [8] E. Saucedo, C.M. Ruiz, V. Bermudez, E. Dieguez, E. Gombia, A. Zappettini, A. Baraldi, N.V. Sochinskii, Photoluminescence and photoconductivity in CdTe crystals doped with bi, *Journal of Applied Physics* 100 (10) (2006) 104901-1–104901-6.
- [9] E. Saucedo, J. Franc, H. Elhadidy, P. Horodysky, C.M. Ruiz, V. Bermudez, N.V. Sochinskii, Investigation of the origin of deep levels in CdTe doped with Bi, *Journal of Applied Physics* 103 (9) (2008) 094901-1–094901-6.
- [10] Y. Seminovski, P. Palacios, P. Wahnón, unpublished results.
- [11] A. Carvalho, A. Tagantsev, S. Oberg, P. Briddon, N. Setter, Intrinsic defects in CdTe and CdZnTe alloys, *Physica B: Condensed Matter* 404 (23–24) (2009) 5019–5021.
- [12] M.A. Berding, Native defects in CdTe, *Physical Review B* 60 (1999) 8943–8950.
- [13] C.K. Egan, Q.Z. Jiang, A.W. Brinkman, Morphology and reconstructions of polar CdTe(111)A,B surfaces by scanning tunneling microscopy, *Journal of Vacuum Science & Technology A* 29 (2011) 011021-1–011021-8.
- [14] D. Mao-Hua, Bismuth-induced deep levels and carrier compensation in CdTe, *Physical Review B* 78 (2008) 172105-1–172105-4.
- [15] H.A. Jahn, E. Teller, Stability of polyatomic molecules in degenerate electronic states. I. Orbital degeneracy, *Proceedings of the Royal Society of London. Series A. Mathematical and Physical Sciences* 161 (905) (1937) 220–235.
- [16] R. Triboulet, P. Siffert, CdTe and Related Compounds; Physics, Defects, Hetero- and Nano-structures, Crystal Growth, Surfaces and Applications: Physics, CdTe-based Nanostructures, Semimagnetic Semiconductors, Defects, European Materials Research Society Series, Elsevier, 2009.
- [17] M. Hage-Ali, I.V. Mitchell, J.J. Grob, P. Siffert, Heavy element diffusion in cadmium telluride, *Thin Solid Films* 19 (1973) 409–418.
- [18] C.S. Fuller, J.A. Ditzenberger, Effect of structural defects in germanium on the diffusion and acceptor behavior of copper, *Journal of Applied Physics* 28 (1957) 40–48.
- [19] G. Kresse, J. Furthmüller, Efficient iterative schemes for *ab initio* total-energy calculations using a plane-wave basis set, *Physical Review B* 54 (1996) 11169–11186.
- [20] G. Kresse, J. Furthmüller, Efficiency of *ab-initio* total energy calculations for metals and semiconductors using a plane-wave basis set, *Computational Materials Science* 6 (1) (1996) 15–50.
- [21] J. Perdew, K. Burke, M. Ernzerhof, Generalized gradient approximation made simple 77 (1996) 3865–3868.
- [22] D.C. Langreth, M.J. Mehl, Beyond the local-density approximation in calculations of ground-state electronic properties, *Physical Review B* 28 (1983) 1809–1834.
- [23] P.E. Blöchl, Projector augmented-wave method, *Physical Review B* 50 (1994) 17953–17979.
- [24] G. Kresse, D. Joubert, From ultrasoft pseudopotentials to the projector augmented-wave method, *Physical Review B* 59 (1999) 1758–1775.
- [25] J. Heyd, G.E. Scuseria, M. Ernzerhof, Hybrid functionals based on a screened coulomb potential, *The Journal of Chemical Physics* 118 (18) (2003) 8207–8215.
- [26] J. Heyd, G.E. Scuseria, M. Ernzerhof, Erratum: hybrid functionals based on a screened Coulomb potential, *Journal of Chemical Physics* 124 (2006) 219906-1.
- [27] I. Aguilera, P. Palacios, P. Wahnón, Optical properties of chalcopyrite-type intermediate transition metal band materials from first principles, *Thin Solid Films* 516 (20) (2008) 7055–7059, Proceedings on Advanced Materials and Concepts for Photovoltaics EMRS 2007 Conference, Strasbourg, France.
- [28] M.-H. Du, H. Takenaka, D.J. Singh, Carrier compensation in semi-insulating CdTe: first-principles calculations, *Physical Review B* 77 (2008) 094122-1–094122-5.